MOLECULAR AND CELLULAR BIOLOGY, Nov. 2005, p. 10040–10051 Vol. 25, No. 22
0270-7306/05/$08.00+0 doi:10.1128/MCB.25.22.10040–10051.2005

Intrinsic Function of the Aryl Hydrocarbon (Dioxin) Receptor as a Key Factor in Female Reproduction

Takashi Baba,[1] Junsei Mimura,[2,4] Naohito Nakamura,[1,4] Nobuhiro Harada,[3] Masayuki Yamamoto,[2] Ken-ichirou Morohashi,[1,4]† and Yoshiaki Fujii-Kuriyama[2,4]*†

Department of Developmental Biology, National Institute for Basic Biology, 5-1 Higashiyama, Myodaiji-cho, Okazaki, Aichi 444-8787, Japan[1]; TARA Center, University of Tsukuba, 1-1-1 Tennoudai, Tsukuba, Ibaraki 305-8577, Japan[2]; Department of Biochemistry, Fujita Health University School of Medicine, 1-98 Dengakugakubo, Kutsukake-cho, Toyoake, Aichi 470-1192, Japan[3]; and Solution Oriented Research for Science and Technology, Japan Science and Technology Agency, 4-1-8 Honcho, Kawaguchi, Saitama 332-0012, Japan[4]

Received 20 May 2005/Returned for modification 2 July 2005/Accepted 3 September 2005

Dioxins exert a variety of adverse effects on organisms, including teratogenesis, immunosuppression, tumor promotion, and estrogenic action. Studies using aryl hydrocarbon receptor (AhR)-deficient mice suggest that the majority of these toxic effects are mediated by the AhR. In spite of the adverse effects mediated by this receptor, the AhR gene is conserved among a number of animal species, ranging from invertebrates to vertebrates. This high degree of conservation strongly suggests that AhR possesses an important physiologic function, and a critical function is also supported by the reduced fertility observed with AhR-null female mice. We demonstrate that AhR plays a crucial role in female reproduction by regulating the expression of ovarian P450 aromatase (*Cyp19*), a key enzyme in estrogen synthesis. As revealed by in vitro reporter gene assay and in vivo chromatin immunoprecipitation assay, AhR cooperates with an orphan nuclear receptor, Ad4BP/SF-1, to activate *Cyp19* gene transcription in ovarian granulosa cells. Administration to female mice of an AhR ligand, DMBA (9,10-dimethyl-1,2-benzanthracene), induced ovarian *Cyp19* gene expression, irrespective of the intrinsic phase of the estrus cycle. In addition to elucidating a physiological function for AhR, our studies also suggest a possible mechanism for the toxic effects of exogenous AhR ligands as endocrine disruptors.

The aryl hydrocarbon receptor (AhR), a member of the growing superfamily of basic helix-loop-helix (bHLH)-PAS transcription factors, functions as an intracellular mediator of xenobiotic signaling pathways (37). AhR was originally discovered to occur in hepatocytes as a transcription factor that binds with high affinity to an environmental contaminant, 2,3,7,8-tetrachlorodibenzo-*p*-dioxin (also referred to as TCDD or dioxin) (49). The molecular properties of AhR as a transcription factor have been elucidated by studies of *CYP1A1* gene expression. Normally, AhR exists in the cytoplasm as part of a complex with Hsp90, XAP2, and p23 (28, 34, 35). Upon binding of xenobiotics, such as TCDD and 3-methylcholanthrene (3MC), the receptor complex translocates into the nucleus, where AhR heterodimerizes with the AhR nuclear translocator (Arnt) (61). Within the nucleus, the AhR/Arnt heterodimer binds to XREs (*x*enobiotic *r*esponsive *e*lements) in the promoters of target genes to activate gene expression. A number of genes encoding drug-metabolizing enzymes, including *CYP1A1* and genes encoding UDP-glucuronosyl transferase and glutathione *S*-transferase, have been identified as targets of AhR (18, 21). Gene disruption studies have also revealed that AhR functions in the toxicological effects of dioxins, such as teratogenesis, immunosuppression, tumor promotion, and estrogenic action (6, 19, 38, 50, 56). Despite promoting these multiple adverse effects, AhR is conserved throughout a number of animal species, from invertebrates to vertebrates (20), suggesting that AhR plays a fundamental role in some physiologic process in addition to mediating the response to xenobiotics.

Ovarian functions are primarily regulated by the hypothalamus-pituitary-gonadal (HPG) axis. Gonadotropin-releasing hormone (GnRH) is discharged from the hypothalamic central nervous system and transported through the portal vascular system to stimulate the gonadotrophs of the anterior pituitary. Subsequently, the anterior pituitary secretes the gonadotropins follicle-stimulating hormone (FSH) and luteinizing hormone (LH) into the venous system. In the ovary, FSH promotes the development of immature follicles, eventually leading to the formation of mature preovulatory follicles. Upon stimulation with LH, the mature follicles rupture, leading to ovulation (52). Through the period of follicular maturation to ovulation, gonadotropins stimulate ovarian steroid synthesis. FSH upregulates expression of the P450 aromatase (*Cyp19*) gene (51), which catalyzes the final step of estrogenesis. Although the genes regulated by estradiol are largely unknown, the involvement of estradiol in folliculogenesis was revealed by the phenotype of *Cyp19* knockout (ArKO) mice (17). Due to impaired synthesis of estradiol, *Cyp19* knockout females displayed severely impaired follicular development, resulting in defective ovulation. Interestingly, ovarian defects similar to those seen with ArKO mice were observed upon simultaneous disruption of the estrogen receptor genes, ERα and ERβ (14).

* Corresponding author. Mailing address: TARA Center, University of Tsukuba, 1-1-1 Tennoudai, Tsukuba, Ibaraki 305-8577, Japan. Phone: 81-29-853-7323. Fax: 81-29-853-7318. E-mail: ykfujii@tara.tsukuba.ac.jp.

† These authors equally contributed to this work.

Our analysis of AhR-deficient mice revealed a phenotype defective in reproduction that was similar, albeit milder, to that seen with ArKO and ERα and ERβ double knockout (ERαβKO) mice. AhR-deficient female mice were subfertile, resulting from impaired folliculogenesis and ovulation. These ovarian defects were likely due to insufficient synthesis of estradiol, consistent with the observation that the *Cyp19* gene is a novel target gene of AhR within the ovary. While the mechanisms by which AhR induces drug-metabolizing enzyme genes in response to exogenous ligands have been extensively studied, the intrinsic function of AhR has remained unknown. In this report, we have identified an intrinsic function for AhR, in which this receptor adjusts ovarian estradiol concentrations by regulating *Cyp19* gene transcription. Based on this novel function for AhR, we propose a molecular mechanism by which the AhR ligands, such as DMBA (9,10-dimethyl-1,2-benzanthracene) and TCDD, also function as endocrine disruptors.

MATERIALS AND METHODS

Fertility assessment. For 3 months, eight $AhR^{+/+}$ and $AhR^{-/-}$ females each were mated with $AhR^{+/+}$ or $AhR^{+/-}$ males. The litter size of each pregnancy, average litter size, and total number of pups were determined. To exclude any effect caused by individual differences in male fertility, two female mice (one $AhR^{+/+}$ and one $AhR^{-/-}$) were housed in the same cage (mating cage) with a single male mouse ($AhR^{+/+}$ or $AhR^{+/-}$). Once known to be pregnant, female mice were isolated until they gave birth. The numbers of pups were counted on the day of bearing. Female mice were returned to mating cages the next day. This experiment continued for 3 months.

Determination of estrus cycle. To determine the estrus cycle phase, vaginal smears were collected by rinsing the vagina with phosphate-buffered saline (PBS) at 1700 h. Collected smears were mounted on glass slides and stained with Giemsa solution. When angular cells or nucleated epithelial cells occupied the majority of the smear, we determined that the mice were in proestrus or estrus. When a multitude of leukocytes were observed, animals were in metestrus or diestrus (42). These observations were performed for 21 consecutive days.

Superovulation. The estrus cycle was induced artificially by intraperitoneal injection of 5 U pregnant-mare serum gonadotropin (PMSG) (Teikoku Zouki, Japan) at 1700 h on day 1 of the experiment and 5 U human chorionic gonadotropin (hCG) (Teikoku Zouki, Japan) at 1700 h on day 3. In this superovulation protocol, follicles developed to the preovulatory stage following PMSG treatment, and ovulation was induced by hCG treatment. Experiments attempting to rescue $AhR^{-/-}$ ovulation required the intraperitoneal injection of β-estradiol (water soluble; Sigma) dissolved in PBS at 1700 h on day 2. Ovulated oocytes were collected from the oviduct and quantified on day 4.

Determination of serum LH concentrations. One hundred microliters of a GnRH agonist, buserelin (Sigma), in vehicle (PBS-0.3% bovine serum albumin) or vehicle alone was injected into the skin behind the necks of ovariectomized $AhR^{+/+}$ and $AhR^{-/-}$ females as described previously (11, 57). One hour after the injection, mice were anesthetized with diethyl ether. After collection of serum samples, serum LH concentrations were determined by radioimmunoassay (SRL, Inc., Japan).

Determination of hormone concentrations. After subjecting mice to the superovulation protocol, we collected ovaries at three time points during the preovulatory period (48 h after PMSG treatment [PMSG + 48 h], hCG + 5 h, and hCG + 8 h). Each ovary was weighed and then homogenized in diethyl ether to a concentration of 10 mg tissue/100 μl methanol. Aliquots (30 μl) of the redissolved materials were subjected to liquid chromatography-mass spectrometry (Applied Biotechnology, Inc., Japan) to determine the concentrations of estradiol and testosterone by comparing intensity values with standard curves made by standard hormones.

Immunohistochemistry. To detect LH, frozen sections (10 μm) were prepared from paraformaldehyde-fixed pituitaries of $AhR^{+/+}$ and $AhR^{-/-}$ mice, embedded in the Tissue-Tek compound (Sakura Finetechnical Co., Ltd., Japan). After being washed in Tris-buffered saline (50 mM Tris-HCl [pH 7.6], 150 mM NaCl) containing 1 mM $CaCl_2$, slides were boiled in 10 mM sodium citrate (pH 6.0) for antigen unmasking (43) and then treated with methanol at −20°C for 30 min. Sections were then incubated with an antibody against the β subunit of LH (Biogenesis) overnight at 4°C, washed, and treated with a biotinylated donkey anti-rabbit immunoglobulin G (Jackson ImmunoResearch Laboratories, Inc.) for 3 h at room temperature. After being washed, sections were developed with horseradish peroxidase-conjugated streptavidin (Nichirei, Japan) and visualized with diaminobenzidine (Nichirei, Japan) for 10 min at room temperature.

To detect AhR and Cyp19, we prepared paraffin sections (5 μm) from paraformaldehyde-fixed ovaries isolated from $AhR^{+/+}$ and $AhR^{-/-}$ females given PMSG and hCG (hCG + 5 h). After deparaffinization, sections were treated with proteinase K (20 μg/ml) (Sigma) to unmask antigen epitopes and then treated with hydrogen peroxide (0.3% H_2O_2 in methanol). Sections were incubated overnight at 4°C with either anti-AhR (generously provided by R. Pollenz) or anti-Cyp19 (22) antibody, washed, and then incubated with biotinylated donkey anti-rabbit immunoglobulin G for 3 h at room temperature. After being washed, sections were incubated with horseradish peroxidase-conjugated streptavidin and visualized with diaminobenzidine for 4 min at room temperature.

ChIP assay. We performed chromatin immunoprecipitation (ChIP) as previously described (46, 48), with the following modifications. Briefly, to fix the chromatin-protein complexes, ovaries isolated from $AhR^{+/+}$ and $AhR^{-/-}$ females treated with PMSG and hCG (hCG + 2 h) were punctured with a needle containing Dulbecco's modified Eagle's medium (DMEM)–Ham F-12 medium–1% FBS with 1% formaldehyde immediately after removal. After fixation was stopped in 125 mM glycine, the suspension of ovarian cells was filtered through a 70-μm cell strainer (Falcon). The isolated granulosa cells were then resuspended in lysis buffer (50 mM HEPES [pH 7.4], 140 mM NaCl, 1 mM EDTA, 10% glycerol, 0.5% NP-40, 0.25% Triton X-100). Nuclei were recovered by centrifugation at 4°C for 30 min. After dissolution in Tris-EDTA (10 mM Tris-HCl [pH 7.4], 0.1 mM EDTA), nuclei were sonicated to shear genomic DNA to approximately 1-kb fragments. Sheared chromatin-DNA complexes were then subjected to immunoprecipitation with either anti-AhR or anti-Ad4BP antibody (41). DNA was extracted from the precipitates by incubation with proteinase K at 65°C, followed by treatment with phenol-chloroform. Presence of the *Cyp19* promoter region was determined by PCR with the appropriate primer sets, indicated below.

Transfection and luciferase assay. The 5′-flanking regions of the human *CYP19* and mouse *Cyp19* genes were inserted into the pGL3-basic vector (Invitrogen) to generate h*CYP19*-3853Luc and m*Cyp19*-5335Luc, respectively. Human embryonic kidney-derived 293 cells were grown in DMEM (Sigma, St. Louis, Mo.) supplemented with 10% fetal bovine serum (FBS) at 37°C in 5% CO_2. Cells were plated at approximately 15% confluence 1 day before transfection. Transfections were conducted in triplicate in 24-well plates by using Lipofectamine Plus (Gibco BRL, Gaithersburg, Md.), according to the manufacturer's protocol. Each well received 500 ng reporter plasmid, 10 ng of the reference pBOS-LacZ vector, and one of various concentrations (0 to 50 ng) of the expression plasmid encoding either AhR, Arnt, the AhR repressor (AhRR) (36), or Ad4BP/SF-1 (39). Cells were treated for 3 h with lipofection reagent in DMEM without serum and then incubated for 48 h in DMEM-10% FBS with or without 3MC (Wako, Japan). Cells were harvested and subjected to luciferase and β-galactosidase assays. All luciferase activities were normalized to the corresponding β-galactosidase activities. Values are represented as the means ± standard deviations (SD) of three independent experiments.

Immunoprecipitation assay. The full-length cDNAs encoding AhR and Ad4BP/SF-1 were inserted into the expression vectors p3×FLAG-CMV-10 (Sigma) and pEGFP-c1 (Clontech) to generate 3×FLAG-AhR and EGFP-Ad4BP, respectively. These plasmids (1 μg) were cotransfected into 293 cells with the expression vector encoding Arnt as described above. An enhanced green fluorescent protein (EGFP) expression vector was included in the transfection as a control. Forty-six hours after transfection, 1 μM of 3MC was added to stimulate nuclear translocation of AhR. After a 2-h incubation, cells were harvested in lysis buffer (50 mM Tris-HCl [pH 8.0], 300 mM NaCl, 1.5 mM $MgCl_2$, 1 mM EDTA, 1% Triton X-100, 10% glycerol) containing 1× Complete protease inhibitor cocktail (Roche) (30). FLAG-tagged and associated proteins were immunoprecipitated from whole-cell extracts (400 μg) by using anti-FLAG M2-agarose affinity gel (Sigma) in immunoprecipitation buffer (50 mM Tris-HCl [pH 8.0], 150 mM NaCl, 1.5 mM $MgCl_2$, 1 mM EDTA, 1% Triton X-100, 10% glycerol) containing 1× Complete protease inhibitor cocktail. Isolated proteins were subjected to immunoblotting with an anti-GFP antibody (MBL, Nagoya, Japan).

PCR conditions. Primer pairs used for semiquantitative reverse transcription-PCR (RT-PCR) were as follows: AhR(fwd), 5′-CGC GGG CAC CAT GAG CAG-3′; AhR(rev), 5′-CTG TAA CAA GAA CTC TCC-3′; AhRR(fwd), 5′-GCT TTC TGT CCT GCG CCT C-3′; AhRR(rev), 5′-GAA GTC CTG CCG GTC ATC C-3′; Cyp19(fwd), 5′-TCA ATA CCA GGT CCT GGC TA-3′; Cyp19(rev), 5′-GTA TGC ACT GAT TCA CGT TC-3′; P450scc(fwd), 5′-CGA ATC GTC CTA AAC CAA GAG-3′; P450scc(rev), 5′-CAC TGA TGA CCC CTG AGA AAT-3′; 3β HSD(fwd), 5′-ACT GCA GGA GGT CAG AGC T-3′;

3β HSD(rev), 5′-GCC AGT AAC ACA CAG AAT ACC-3′; P450 17α(fwd), 5′-GGG GCA GGC ATA GAG ACA ACT-3′; P450 17α(rev), 5′-GGG TGT GGG TGT AAT GAG ATG-3′; $P27^{kip1}$(fwd), 5′-AAG CGG ATC ACC CCA AGC CT-3′; $P27^{kip1}$(rev), 5′-GTT GGC GGT TTT GTT TTG CG-3′; C/EBPβ(fwd), 5′-TCT ACT ACG AGC CCG ACT GCC T-3′; C/EBPβ(rev), 5′-AGCTTG TCC ACC GTC TTC TT-3′; GAPDH(fwd) (GAPDH, glyceraldehyde-3-phosphate dehydrogenase), 5′-GGC ATG GCC TTC CGT GTT CCT-3′; GAPDH(rev), TCC TTG CTG GGG TGG GTG GTC-3′; β-actin(fwd), 5′-ATG GAT GAC GAT ATC GCT-3′; and β-actin(rev), 5′-ATG AGG TAG TCT GTC AGG T-3′. Thermal-cycling conditions were as follows: 28 cycles of 30 s at 94°C, 30 s at 60°C, and 1 min at 72°C for the amplification of AhR, $P27^{kip1}$, and C/EBPβ; 32 cycles of 30 s at 94°C, 30 s at 58°C, and 1 min at 72°C for AhRR; 25 cycles of 30 s at 94°C, 30 s at 60°C, and 1 min at 72°C for Cyp19, P450scc, 3β HSD, and P450 17α; and 22 cycles of 30 s at 94°C, 30 s at 60°C, and 1 min at 72°C for GAPDH and β-actin. Quantitative RT-PCR was performed with a TaqMan gene expression assay (Applied Biosystems) on a 7500 real-time PCR system (Applied Biosystems). Thermal-cycling conditions were 50 cycles of 15 s at 95°C and 1 min at 60°C.

Primer pairs used for ChIP assays were as follows: XRE of Cyp19 (fwd), TGA GAG TGA ACT GCA GGA AG-3′; XRE of Cyp19 (rev), ACC TCA TGG CTA AGG CAA TG-3′; Ad4 of Cyp19 (fwd), ATA AGG AGG ATT GCC TCA GC-3′; Ad4 of Cyp19 (rev), GCT CCT GTC ACT TGG AAG GG-3′; −2740∼−2441 of Cyp19 (fwd), GAC TTT GCA TAG AGA CTT GG-3′; −2740∼−2441 of Cyp19 (rev), CTG TTT AGT GTT GTC AAT GC-3′; β-actin(fwd), AGG GTG TGA TGG TGG GAA TGG-3′; and β-actin(rev), TGG CTG GGG TGT TGA AGG TCT-3′. Thermal-cycling conditions were 32 cycles of 30 s at 94°C, 30 s at 62°C, and 1 min at 72°C.

RESULTS

Phenotype of $AhR^{-/-}$ females related to reproduction. The reproductive defects of $AhR^{-/-}$ females have remained controversial (1). We therefore examined if fertility was impaired in the $AhR^{-/-}$ females used in this study. To avoid experimental variation due to genetic background, we used AhR knockout (AhR KO) mice backcrossed to C57BL/6J mice for more than eight generations. For 3 months, $AhR^{+/+}$ and $AhR^{-/-}$ females were mated with $AhR^{+/+}$ or $AhR^{+/-}$ males, and the number of pups delivered was counted. Using eight randomly selected $AhR^{+/+}$ and $AhR^{-/-}$ females, the total number of pups delivered by the $AhR^{+/+}$ females was 213, while those delivered by $AhR^{-/-}$ females was 57 (Table 1). The average litter size of $AhR^{-/-}$ females was approximately 40% that of the wild type. None of the $AhR^{-/-}$ females examined bore a third litter, and one of these mutant animals was unable to deliver pups during the mating period. Although levels of reproductive activity varied among individuals, these results clearly indicated a decreased fertility of $AhR^{-/-}$ females.

To explore the causes of $AhR^{-/-}$ subfertility, we histologically examined the reproductive organs. Examination of the organs revealed a reduction of the ratio of ovarian weight to body weight in the $AhR^{-/-}$ females to 56% of that seen in the wild-type animals (0.055 ± 0.010% for $AhR^{+/+}$ versus 0.031 ± 0.003% for $AhR^{-/-}$, $n = 3$, $P < 0.05$). In contrast, the uterus appeared to be unaffected (0.272 ± 0.030% for $AhR^{+/+}$ versus 0.294 ± 0.049% for $AhR^{-/-}$, $n = 3$) (Fig. 1A and B). Based on histological analyses, the ovaries of $AhR^{-/-}$ animals developed follicles up to the antral/preovulatory stage in the presence of slightly hypoplastic interstitial cells (Fig. 1C). The corpus luteum, however, was barely detectable in $AhR^{-/-}$ ovaries. As the corpora lutea develop from postovulatory follicles, this observation implied a failure in a final step of follicular maturation and/or ovulation.

As failures of follicular maturation and ovulation are frequently accompanied by a disordered estrus cycle (29, 58), we then examined if the ovarian estrus cycle proceeds normally in $AhR^{-/-}$ mice (Fig. 1D). In wild-type and $AhR^{+/-}$ mice, the estrus cycle progressed regularly, lasting 4 to 5 days. Although we observed considerable individual variation, $AhR^{-/-}$ females displayed significantly disordered estrus cycles (Fig. 1D), which we classified into three groups. Mice in group I showed a prolonged cycle. In group II, animals exhibited a cycle that was irregularly shortened or prolonged. Unusually prolonged estrus phases were observed for mice classified as group III. Such irregularities were not observed for $AhR^{+/+}$ or $AhR^{+/-}$ mice.

As the HPG axis is crucial for progression of the estrus cycle, we examined the tissues of the HPG axis to determine which region is affected in $AhR^{-/-}$ animals. First, we examined the ability of the ovaries of $AhR^{-/-}$ mice to respond to gonadotropins. $AhR^{-/-}$ females aged 3 and 12 weeks were subjected to a standard superovulation protocol, and the numbers of ovulated oocytes in response to gonadotropin stimulation were counted. In $AhR^{-/-}$ mice, the total number of the ovulated oocytes decreased to approximately one-sixth the level seen for age-matched wild-type females (Table 2). We then examined the production of gonadotropins in the pituitaries of $AhR^{-/-}$ animals by immunohistochemical analysis using an anti-LH antibody (Fig. 2A). LH-immunoreactive gonadotrophs were present in the anterior lobes of the pituitary glands of both $AhR^{-/-}$ and $AhR^{+/+}$ mice. We then investigated the ability of gonadotrophs to secrete LH in response to stimulation with a GnRH agonist, buserelin (des-Gly_{10}-[D-Ser{t-Bu}$_6$]-LH-RH ethylamide). To exclude any feedback effects from the ovaries, animals were ovariectomized prior to experimentation. After subcutaneous injection of buserelin into the ovariectomized mice, we determined the serum LH concentrations. Neither the basal nor the buserelin-induced concentrations differed between $AhR^{+/+}$ and $AhR^{-/-}$ mice, indicating that the ability of $AhR^{-/-}$ gonadotrophs to se-

TABLE 1. Distribution of pups by female genotype

Genotype		No. of pups per litter				Total pups[b]
Female	Male	1st	2nd	3rd	Avg[a]	
$AhR^{+/+}$	$AhR^{+/-}$	8	11	10	9.7	29
		8	11		9.5	19
		10	10		10.0	20
		9	11	9	9.7	29
$AhR^{+/+}$	$AhR^{+/+}$	11	13	11	11.7	35
		9	10	11	10.0	30
		9	10	10	9.7	29
		11	11		11.0	22
$AhR^{-/-}$	$AhR^{+/-}$	4	5		4.5	9
		8			8.0	8
		3	5		4.0	8
						0
$AhR^{-/-}$	$AhR^{+/+}$	2	1		1.5	3
		2	3		2.5	5
		7	3		5.0	10
		10	4		7.0	14

[a] Average litter sizes for all $AhR^{+/+}$ females and $AhR^{-/-}$ females were 10.1 and 4.4, respectively.

[b] Total numbers of pups for all $AhR^{+/+}$ females and $AhR^{-/-}$ females were 213 and 57, respectively.

A

	total body (g)	ovary (mg)	ovary / body (%)	uterus (mg)	uterus / body (%)
AhR (+/+)	24.9	13.1 (5.6 + 7.5)	0.053	75.4	0.303
AhR (+/+)	23.1	10.6 (5.2 + 5.4)	0.046	56.3	0.244
AhR (+/+)	24.3	16.0 (8.2 + 7.8)	0.066	65.3	0.269
AhR (–/–)	22.0	7.1 (3.3 + 3.8)	0.032	72.9	0.331
AhR (–/–)	24.1	8.0 (3.2 + 4.8)	0.033	57.6	0.239
AhR (–/–)	21.5	5.8 (3.2 + 2.6)	0.027	67.2	0.313

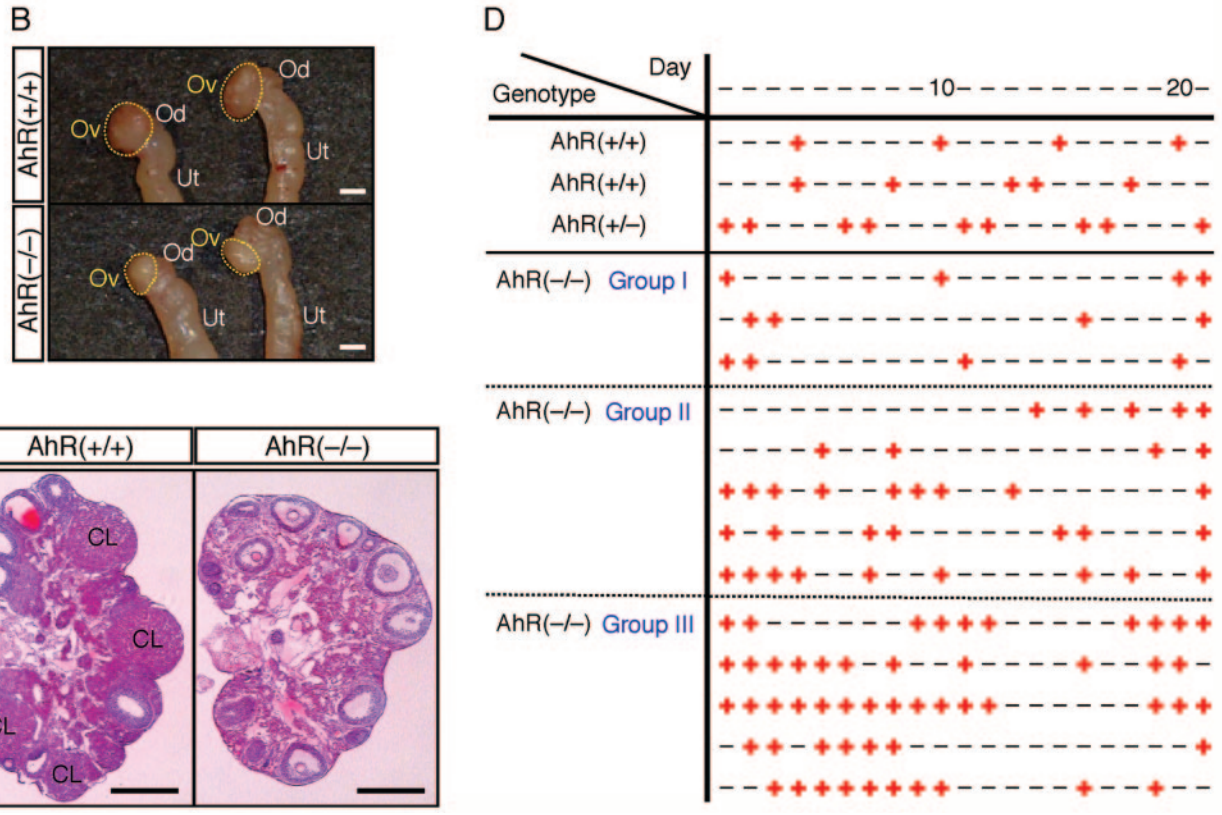

FIG. 1. Estrus cycle and folliculogenesis affected in $AhR^{-/-}$ ovaries. (A) Ovarian and uterine wet weights of $AhR^{+/+}$ and $AhR^{-/-}$ females. The ovaries and uteri isolated from 9-week-old mice were weighed. The ratios of ovarian or uterine wet weight to total body weight are also indicated. Three $AhR^{+/+}$ and $AhR^{-/-}$ mice each were examined in this experiment. (B) Morphologies of the reproductive tracts of 9-week-old $AhR^{+/+}$ and $AhR^{-/-}$ females. The ovaries are outlined in broken yellow lines. Ov, Od, and Ut indicate the ovary, oviduct, and uterus, respectively. Bar, 1 mm. (C) Histological analysis of the ovaries of $AhR^{+/+}$ and $AhR^{-/-}$ mice. Five-micrometer paraffin-embedded sections of $AhR^{+/+}$ and $AhR^{-/-}$ ovaries were stained with hematoxylin-eosin. CL indicates the corpus luteum. Bar, 0.5 mm. (D) Disordered estrus cycles in $AhR^{-/-}$ females. Vaginal smears from $AhR^{+/+}$, $AhR^{+/-}$, and $AhR^{-/-}$ female mice were collected for 21 consecutive days and stained with Giemsa solution. +, proestrus or estrus; −, metestrus or diestrus.

crete gonadotropins in response to upstream signals was not impaired (Fig. 2B). These results strongly suggest that the reduced fertility of $AhR^{-/-}$ females was due primarily to ovarian defects.

Synthesis of estradiol in $AhR^{-/-}$ ovaries is insufficient compared with that of the wild type. Estradiol is an essential sex hormone for female reproduction, and serum concentrations increase transiently during the preovulatory stage (54). We measured the concentrations of estradiol in the ovaries at three time points during the preovulatory stage (Fig. 3A). As $AhR^{-/-}$ females failed to demonstrate normal estrus cycles,

TABLE 2. Numbers of ovulated oocytes according to female genotype

Genotype	Age (wk)	No. of ovulated oocytes (mean ± SD)	No. of mice
$AhR^{+/+}$	3	51.3 ± 2.2	4
	12	25.0 ± 1.0	3
$AhR^{-/-}$	3	8.7 ± 8.5	3
	12	4.0 ± 4.6	3

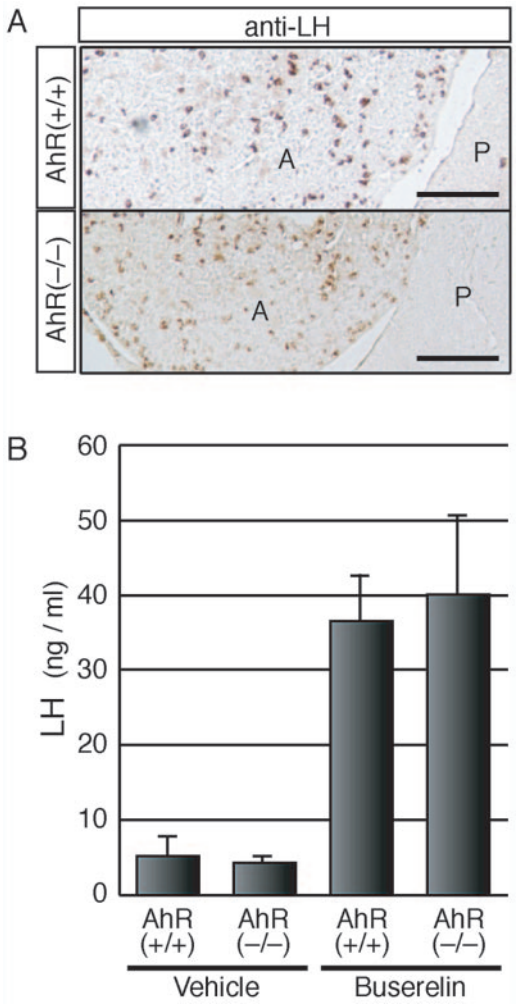

FIG. 2. Functionally normal gonadotropes of AhR$^{-/-}$ pituitaries. (A) Presence of gonadotrophs in the pituitary anterior lobes of AhR$^{-/-}$ females. Cryosections of pituitaries isolated from AhR$^{+/+}$ and AhR$^{-/-}$ mice were treated with an anti-LH antibody, which should specifically stain pituitary gonadotrophs. A and P represent the anterior and posterior lobes, respectively. Bar, 0.1 mm. (B) Secretion of LH from the gonadotrophs of AhR$^{-/-}$ pituitaries. A GnRH agonist, buserelin (2 μg), or vehicle alone was injected subcutaneously into ovariectomized AhR$^{+/+}$ and AhR$^{-/-}$ females. One hour after injection, serum levels of LH were determined. Values are represented as means ± SD for three to four mice.

we forced the estrus cycle to proceed by gonadotropin stimulation. In AhR$^{-/-}$ females, the concentrations of intraovary estradiol were decreased to 20 to 30% of the levels seen for wild-type animals at all three time points (Fig. 3B). Testosterone, the precursor of estradiol, was slightly increased in the ovaries of AhR$^{-/-}$ mice in comparison with the concentrations observed for AhR$^{+/+}$ females (Fig. 3C). These observations suggest that the decreases in ovarian estradiol are responsible for the reproductive defects of AhR$^{-/-}$ females. We therefore reasoned that an intraperitoneal injection of estradiol at the appropriate time of the ovulatory cycle would rescue the observed phenotype. AhR$^{-/-}$ mice were treated at day 2 with estradiol in the superovulation protocol (Fig. 3D), and then released oocytes were quantified. Administration of up to 10 ng estradiol to AhR$^{-/-}$ mice partially corrected the decrease in the number of ovulated oocytes in a dose-dependent manner. Administration of 20 ng estradiol failed to increase the number of ovulated oocytes further (Fig. 3E). Although these results clearly indicate that insufficient estradiol at least contributes to AhR$^{-/-}$ subfertility, either the timing or the site of estradiol administration may not have been optimal for full recovery of fertility. Additional factors may also be affected with AhR$^{-/-}$ mice, influencing the reproduction process.

AhR is indispensable for proper expression of the *Cyp19* gene in the ovary. As AhR functions as a transcription factor, the above observations suggested that this receptor is involved in the transcriptional regulation of steroidogenic genes. The expression pattern of AhR during folliculogenesis, however, is largely unknown. We therefore examined AhR expression throughout an artificially produced estrus cycle in wild-type mice (Fig. 4A). AhR mRNA was expressed throughout the preovulatory period. AhRR, a target of AhR transcriptional regulation, represses AhR function (2, 36). Interestingly, the expression of AhRR was upregulated at 6 and 7 h after hCG injection (Fig. 4B), suggesting that, while AhR becomes functionally active after treatment with PMSG, its activity thereafter is repressed by the action of AhRR. We therefore examined the expression of the *Cyp19* gene, whose product is essential for estradiol production, during folliculogenesis. *Cyp19* gene expression was activated 48 h after PMSG treatment and downregulated gradually after hCG treatment. This downregulation appeared to coincide with the induction of AhRR expression.

We then compared the expression levels of other steroidogenic enzymes within the ovaries of wild-type and AhR$^{-/-}$ mice at 4 and 7 h after hCG treatment (Fig. 4C). We did not observe any alteration in expression of mRNAs encoding steroidogenic Cyp11A (P450scc), 3β HSD, and Cyp17 (P450 17α, 17α-hydroxylase) between wild-type and knockout animals at the two time points examined. While Cyp19 mRNA was potently upregulated in wild-type ovaries during the final maturation stage of folliculogenesis induced by hormone treatment (Fig. 4B), expression of this gene was markedly reduced in AhR$^{-/-}$ ovaries, even at 4 h after hCG treatment. Quantitative RT-PCR demonstrated that the expression of Cyp19 in AhR$^{-/-}$ females was reduced by greater than 90% from that of wild-type animals 4 h after hCG treatment (Fig. 4D), indicating that Cyp19 mRNA expression was not upregulated in AhR$^{-/-}$ ovaries during hormone treatment. There were no detectable differences between the wild-type and AhR knockout mice in the expression of either p27^{kip1} or C/EBPβ, both of which are involved in ovulation (16, 29, 47, 58). As expected, there was no expression of AhRR mRNA in AhR$^{-/-}$ ovaries at 7 h after hCG treatment. To determine if Cyp19 protein levels were also altered in AhR$^{-/-}$ ovaries, we prepared whole-tissue extracts from hormone-treated ovaries (hCG + 5 h) and subjected these samples to Western blot analysis with an anti-Cyp19 antibody. In agreement with the results of our mRNA expression analysis, we detected decreased levels of Cyp19 protein in the ovaries of AhR$^{-/-}$ mice (Fig. 4E). Consistent with previous reports (53, 62), immunohistochemical staining with anti-AhR and anti-Cyp19 antibodies demonstrated coexpression of AhR and Cyp19 in the granulosa cells of antral follicles (Fig. 4F). We also confirmed by immunohis-

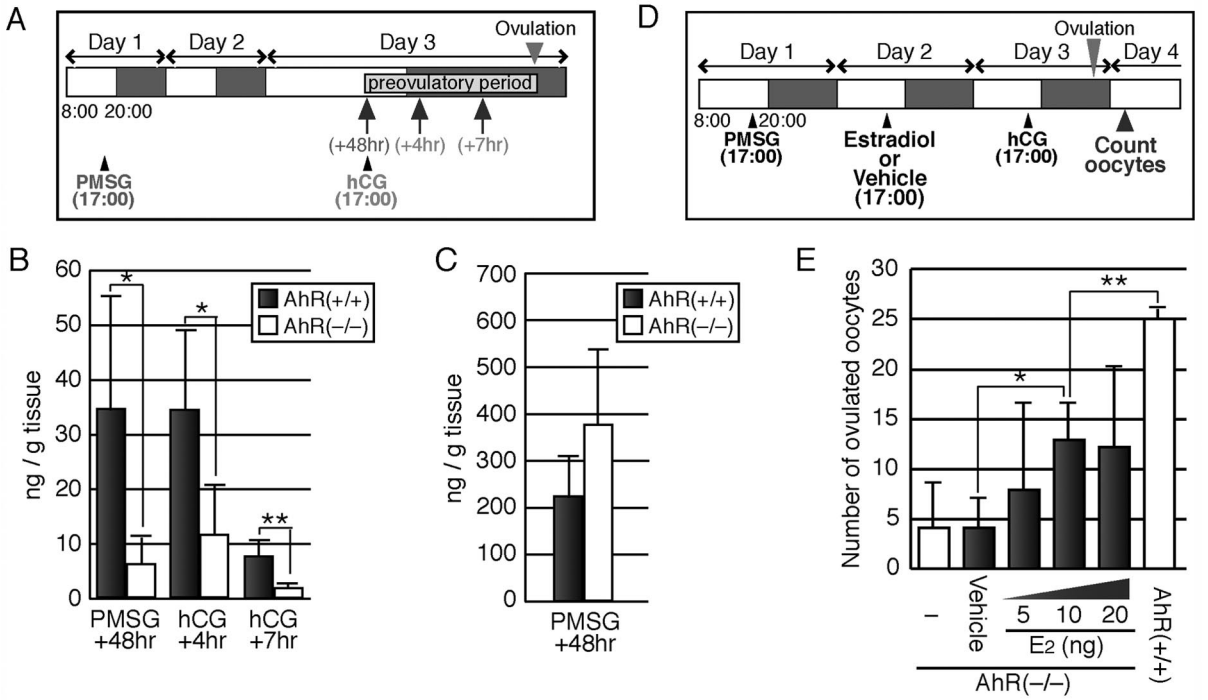

FIG. 3. Concentrations of intraovarian steroids in $AhR^{-/-}$ females and the rescue of ovulation by estradiol treatment. (A) Schematic representation of the experimental procedure used to determine intraovarian steroid concentrations during the preovulatory period. (B) Intraovarian estradiol concentrations in $AhR^{+/+}$ and $AhR^{-/-}$ females. The ovaries of at least three $AhR^{+/+}$ and three $AhR^{-/-}$ female mice were collected at the times indicated in panel A. Estradiol concentrations were then determined by liquid chromatography-mass spectrometry analysis. *, $P < 0.10$; **, $P < 0.05$. (C) Intraovarian testosterone concentrations were determined as described for panel B. (D) Schematic representation of the experimental estradiol administration procedure used to rescue the ovulation of $AhR^{-/-}$ mice. Mice treated with PMSG at day 1 were divided into two groups. One group was treated with various quantities of estradiol, while the other group was given vehicle alone on day 2. The mice from both groups were treated with hCG on day 3, and ovulation was assessed at day 4. (E) Effects of estradiol administration on ovulation in $AhR^{-/-}$ females. After the treatment of $AhR^{+/+}$ and $AhR^{-/-}$ females with PMSG and hCG, the oocytes released by ovulation were counted (open bars). $AhR^{-/-}$ females were also given an intraperitoneal injection of 5 to 20 ng 17β-estradiol (E2) or vehicle alone (filled bars) as described for panel D prior to counting the ovulated oocytes. *, $P < 0.025$; **, $P < 0.005$.

tochemistry that Cyp19 protein levels were diminished in the granulosa cells of $AhR^{-/-}$ ovaries (Fig. 4F).

AhR directly activates *Cyp19* gene transcription in cooperation with an orphan nuclear receptor, Ad4BP/SF-1. As the previously described results strongly suggest the involvement of AhR in *Cyp19* expression, we examined the mechanism by which AhR regulated *Cyp19* gene transcription. The *Cyp19* gene has multiple tissue-specific first exons (23, 33, 55). In the ovary, this gene is transcribed from exon PII (Ex 1d) in a mechanism involving the orphan nuclear receptor Ad4BP/SF-1 (8, 32, 40, 45). The binding site for Ad4BP/SF-1 is conserved within the 5′ upstream regions of the human and mouse genes. We also determined that the human *CYP19* and mouse *Cyp19* genes have an AhR/Arnt-binding sequence (XRE) 3,756 and 5,058 bp upstream of the ovary-specific first exon, respectively (Fig. 5A and B). We therefore transiently transfected the expression vectors of AhR, Arnt, and Ad4BP/SF-1 into cultured cells to investigate the promoter function of the *CYP19*/*Cyp19* genes. While Ad4BP/SF-1 clearly activated *CYP19*/*Cyp19* gene transcription, cotransfection of AhR and Arnt resulted in only weak activation. Simultaneous expression of AhR/Arnt with Ad4BP/SF-1, however, synergistically activated the Cyp19 promoter (Fig. 5C and D). Subsequent expression of AhRR suppressed the transcription activation induced by AhR (Fig. 5C and D).

The observed synergistic activation of the *CYP19*/*Cyp19* promoter by AhR/Arnt and Ad4BP/SF-1 implied a physical interaction between these proteins. To verify this interaction, we cotransfected expression vectors encoding 3×FLAG-AhR, Arnt, and EGFP-Ad4BP/SF-1 and then attempted to coimmunoprecipitate these components by using an anti-FLAG antibody. EGFP-Ad4BP/SF-1, but not EGFP, was coimmunoprecipitated with FLAG-AhR (Fig. 6A), indicating a potential physical interaction between AhR/Arnt and Ad4BP/SF-1. To investigate if AhR binds to the XRE within the promoter of *Cyp19* in vivo, we performed a ChIP assay using chromatin isolated from the granulosa cells of gonadotropin-treated ovaries (Fig. 6B). PCR analysis of the immunoprecipitates isolated using an anti-AhR antibody (Fig. 6B) revealed that the XRE of the *Cyp19* gene was associated with AhR in samples derived from wild-type mice but not $AhR^{-/-}$ mice (Fig. 6C). This result clearly indicates that AhR was recruited to the *Cyp19* promoter in vivo. As the *Cyp19* gene is synergistically activated by AhR/Arnt and Ad4BP/SF-1, we assumed that AhR, Arnt, and Ad4BP/SF-1 physically interact on the *Cyp19* promoter. We next examined whether anti-AhR antibodies precipitate

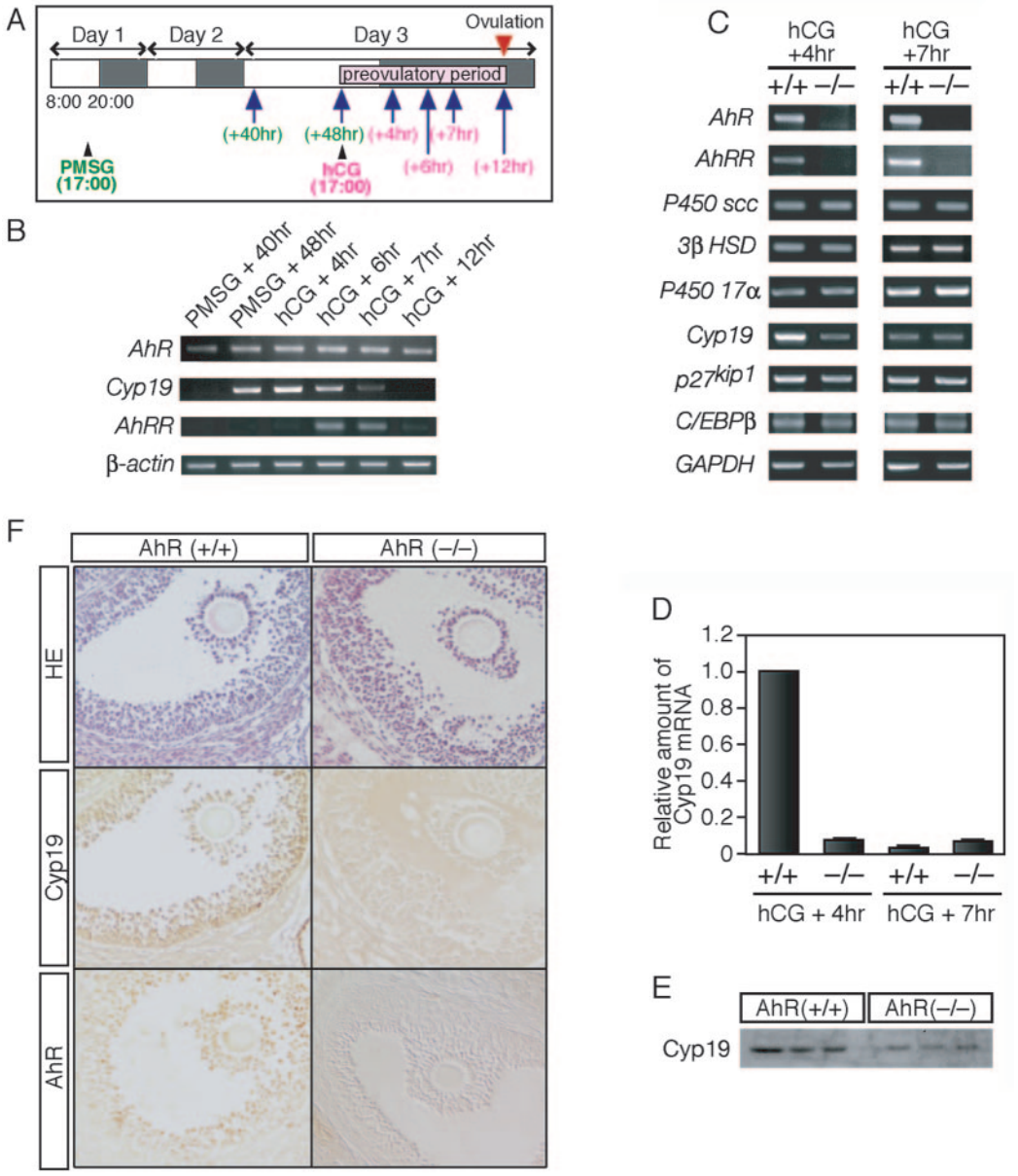

FIG. 4. AhR regulates the expression of ovarian *Cyp19* during the preovulatory period. (A) Schematic representation of the experimental procedure. The estrus cycle was induced artificially by intraperitoneal injection of PMSG at 1700 h on day 1 and of hCG at 1700 h on day 3. Ovaries were collected 40 and 48 h after PMSG injection or 4, 6, 7, and 12 h after hCG injection (indicated by arrows). (B) Profiles of mRNA expression for AhR, AhRR, and Cyp19 during the preovulatory period. Total RNA samples, prepared from ovaries derived from hormone-treated mice at the indicated times (top), were subjected to RT-PCR with primers sets specific for AhR, AhRR, and Cyp19. β-Actin mRNA was used as a control. (C) Expression of mRNAs encoding steroidogenic enzymes and proteins involved in ovarian folliculogenesis. Total RNA samples, prepared from the ovaries of hormone-treated $AhR^{+/+}$ and $AhR^{-/-}$ mice at the indicated times (top), were used for RT-PCR with the PCR primers. (D) Quantification of Cyp19 mRNA levels. Total RNA samples, prepared from the ovaries isolated 4 and 7 h after hCG injection, were subjected to quantitative RT-PCR analyses. Three animals were used for this experiment. (E) Expression of Cyp19 protein within $AhR^{+/+}$ and $AhR^{-/-}$ ovaries during the preovulatory period. Whole-cell extracts (10 μg), prepared from the ovaries of hormone-treated (hCG + 5 h) mice, were subjected to Western blot analysis with an anti-Cyp19 antibody. Three $AhR^{+/+}$ and three $AhR^{-/-}$ animals were used for these experiments. (F) Immunohistochemical staining of Cyp19 and AhR in the granulosa cells of $AhR^{+/+}$ and $AhR^{-/-}$ ovaries. Five-micrometer paraffin sections were prepared from the ovaries of hormone-treated (hCG + 5 h) mice. Sections were stained with hematoxylin-eosin (HE) or with anti-AhR or anti-Cyp19 antibody.

the Ad4 site of the *Cyp19* promoter and whether the anti-Ad4BP/SF-1 antibody reciprocally precipitates the XRE sequence. Both the XRE- and Ad4-containing sequences of the *Cyp19* promoter were recovered in both anti-Ad4BP/SF-1 and anti-AhR immunoprecipitates (Fig. 6D). As a control, the sequence between bp −2740 and −2441 was not recovered in either the anti-AhR or the anti-Ad4BP/SF-1 immunoprecipitate, excluding the possibility that incomplete fragmentation of

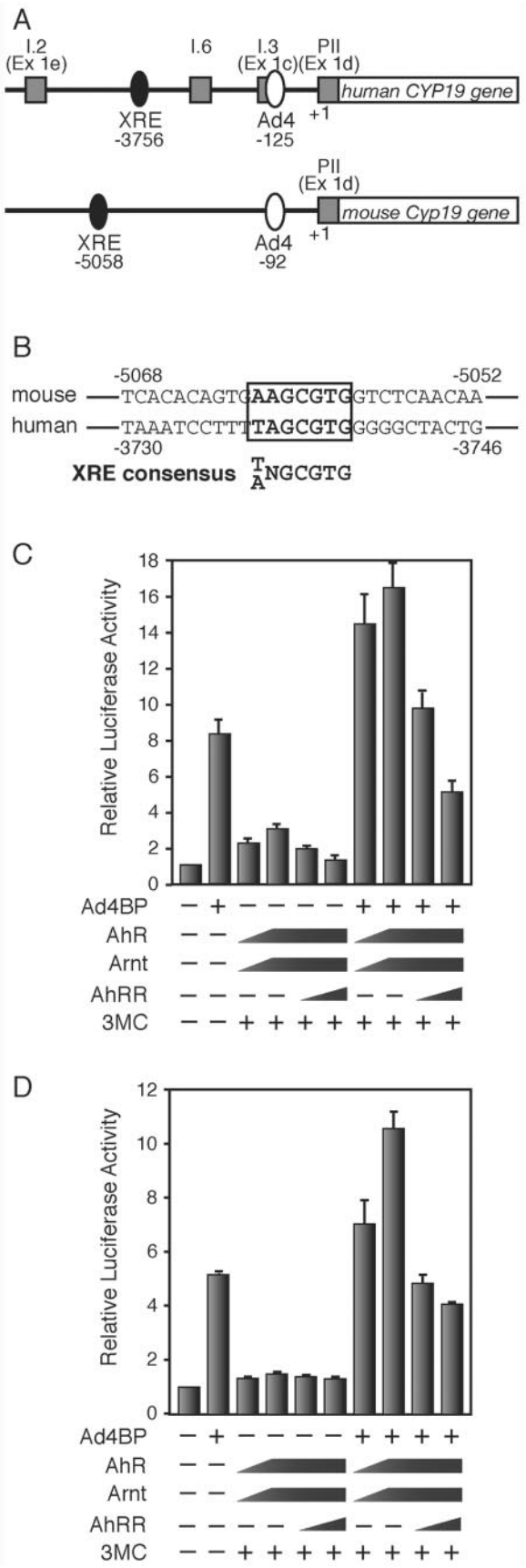

DNA during chromatin preparation resulted in artifactual coimmunoprecipitation of the Ad4- and XRE-containing sequences. To confirm the interaction between AhR and Ad4BP/SF-1 on the *Cyp19* promoter, we investigated whether the XRE is coimmunoprecipitated with Ad4BP/SF-1 in the $AhR^{-/-}$ chromatin (Fig. 6E). Anti-Ad4BP antibody failed to precipitate the XRE-containing sequence in the absence of AhR, indicating that Ad4BP/SF-1 does not bind directly to the XRE but binds indirectly through interaction with the XRE-bound AhR. In addition, we investigated whether AhR knockout affects Ad4BP/SF-1 binding to the Ad4 site and found that there is no difference in binding of Ad4BP/SF-1 between $AhR^{+/+}$ and $AhR^{-/-}$ mice (Fig. 6E). These results clearly demonstrated that both AhR and Ad4BP/SF-1 bind to their cognate binding sites within the *Cyp19* promoter and physically interact, probably leading to cooperative enhancement of *Cyp19* expression.

AhR ligands exerted an estrogenic effect by aberrantly activating *Cyp19* gene expression. While *Cyp19* is expressed transiently at a particular time point in the preovulatory period, AhR is constitutively expressed in granulosa cells. Inadvertently introduced AhR ligands may exert an estrogenic effect by aberrantly upregulating *Cyp19* expression in the ovary. To examine this possibility, we administered DMBA, an AhR ligand, to randomly selected female mice regardless of estrus cycle phase. After a 5-h treatment, we examined the expression of Cyp19 mRNA in the ovary. In a normal estrus cycle, expression of Cyp19 and the resultant estradiol production are induced transiently at proestrus. We observed that Cyp19 mRNA accumulated at proestrus but not at other phases of the estrus cycle in the ovaries of wild-type female mice (Fig. 7A and B). DMBA effectively induced *Cyp19* expression at most of the cycle phases except for metestrus. This reagent, however, failed to induce *Cyp19* gene expression in the ovaries of $AhR^{-/-}$ mice. Thus, AhR appears to have the potential to activate *Cyp19* gene transcription inappropriately in response to exogenous ligands, even when intrinsic estrogen synthesis should not be stimulated.

FIG. 5. Cooperative activation of AhR and Ad4BP/SF-1 on the *Cyp19*/*CYP19* promoter. (A) Schematic representation of the mouse *Cyp19* and human *CYP19* gene promoter regions. The square boxes indicate the first exons, exons I.2 (Ex 1e), I.6, I.3 (Ex 1c), and PII (Ex 1d), expressed specifically in the placenta, bone, adipose tissue, and ovary, respectively. The filled and open ovals represent the AhR/Arnt-binding (XRE) and Ad4BP/SF-1-binding (Ad4) sequences, respectively. The ovary-specific transcription start site is numbered as +1, and the positions of the XRE and Ad4 sites were numbered as the negative values of their distances from the transcription start site. (B) Nucleotide sequences containing the XRE site from the mouse *Cyp19* and human *CYP19* gene upstream regions. The consensus XRE sequence is indicated in bold letters. (C) Cooperative activation of AhR and Ad4BP/SF-1 on the human *CYP19* gene promoter. Expression plasmids encoding AhR, Arnt, AhRR, and Ad4BP/SF-1 were cotransfected into 293 cells with a reporter plasmid, in which luciferase expression is driven by the *CYP19* promoter (h*CYP19*-3853Luc), in the presence (+) or absence (−) of 3MC. After a 48-h incubation, cells were recovered and subjected to luciferase assays. All values are the means ± SD for three experiments. (D) Cooperative activation of AhR and Ad4BP/SF-1 on the mouse *Cyp19* promoter. m*Cyp19*-5335Luc was used for this assay. All other conditions were as specified for panel C.

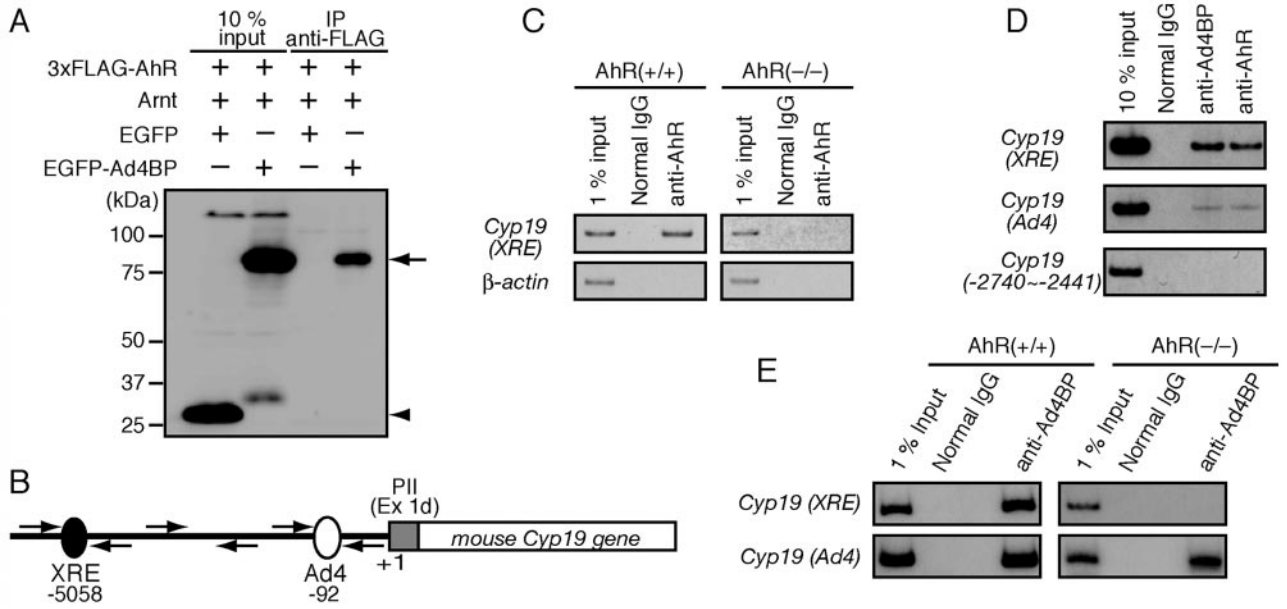

FIG. 6. Interaction of AhR with Ad4BP/SF-1 on the *Cyp19* promoter. (A) Detection of a physical interaction between AhR and Ad4BP/SF-1 by coimmunoprecipitation. FLAG-tagged proteins from whole-cell extracts of 293 cells transfected with 3×FLAG-AhR, Arnt, and EGFP-Ad4BP were immunoprecipitated (IP) with an anti-FLAG antibody. The immunoprecipitates were then subjected to immunoblotting with an anti-GFP antibody. An EGFP expression vector was transfected as a control. An arrow and an arrowhead indicate the EGFP-Ad4BP and EGFP samples, respectively. (B) Schematic representation of the location of primers used in the ChIP assays. Three sets of primers were used to amplify DNA regions containing the XRE site at −5058 and the Ad4/SF-1 sequence at −92 and a third unrelated region (−2740 to −2441), containing neither of them, as a control. (C) Binding of AhR to the promoter region of the *Cyp19* gene, revealed by ChIP assays. Soluble chromatin, prepared from preovulatory granulosa cells (hCG + 2 h), was subjected to ChIP assay with an anti-AhR antibody. β-Actin was used as a negative control. (D) Interaction between AhR and Ad4BP/SF-1 on the *Cyp19* gene promoter. Chromatin isolated from preovulatory granulosa cells was incubated with anti-AhR or anti-Ad4BP/SF-1 antibody and then subjected to PCR with two sets of primers amplifying the XRE and Ad4 sites. A primer pair specific for the sequence from −2740 to about −2441 was used as a control. (E) Binding of Ad4BP/SF-1 to the XRE and Ad4 sites in the presence or absence of AhR, revealed by ChIP assays. Chromatin isolated from preovulatory granulosa cells of the $AhR^{+/+}$ and $AhR^{-/-}$ ovaries was incubated with anti-Ad4BP/SF-1 or control antibody and then subjected to PCR to amplify the XRE and Ad4 sites. IgG, immunoglobulin G.

DISCUSSION

In agreement with a previous report (1), $AhR^{-/-}$ females demonstrated compromised fertility. The number of delivered pups was clearly decreased in comparison to those delivered by wild-type animals. As the phenotype of *AhR* gene disruption suggested a novel physiological function for AhR, in addition to its well-established xenobiotic metabolizing function, we investigated the molecular mechanisms underlying defective fertility in $AhR^{-/-}$ female mice.

Reproductive defects seen with $AhR^{-/-}$ female are primarily due to insufficient synthesis of estradiol in the ovary. Abbott et al. described that $AhR^{-/-}$ females exhibited difficulties in maintaining conceptuses during pregnancy (1), while Benedict et al. reported that AhR deficiency affected follicular maturation and ovulation under normal growth conditions (3, 4). Our studies indicated that follicles present in the ovaries of $AhR^{-/-}$ mice developed to an antral/preovulatory stage, while the corpus luteum was barely detectable. Upon stimulation of superovulation, the number of ovulated oocytes in $AhR^{-/-}$ females was significantly lower than those seen with the wild type. In conjunction with the observations of Benedict et al., these results suggested that the reduced fertility of $AhR^{-/-}$ females was a consequence of ovarian defects during the period of late folliculogenesis to follicular rupture.

Both implantation and follicular maturation are highly dependent on estrogenic action (12). The phenotype of $AhR^{-/-}$ mice suggested the hypothesis that the observed reproductive failure might be induced by the disruption of genes involved in estrogen production or action. The ovaries of ArKO mice were reported to contain many large follicles filled with granulosa cells, with an absence of a corpus luteum (17). ERαβKO female mice (14), completely lacking a receptor-mediated response to estrogen, failed to induce preovulatory follicle formation after superovulation treatment. The female reproduction defects of ArKO and ERαβKO mice resembled those of AhR KO mice, albeit with a more severe phenotype. The similarities between these phenotypes strongly suggested that AhR KO mice have deficits in estrogen production or action. After hypothesizing that estradiol production in the preovulatory period was affected in AhR KO females, we determined that intraovarian estrogen concentrations during the preovulatory stages were decreased in $AhR^{-/-}$ females. Administration of estradiol increased the number of ovulated oocytes in $AhR^{-/-}$ females, suggesting that the subfertility of $AhR^{-/-}$ mice results primarily from reduced levels of ovarian estrogen.

***Cyp19* gene transcription mediated synergistically by AhR and Ad4BP/SF-1.** Ovarian sex steroids, such as estrogen and progesterone, are synthesized from cholesterol through multi-

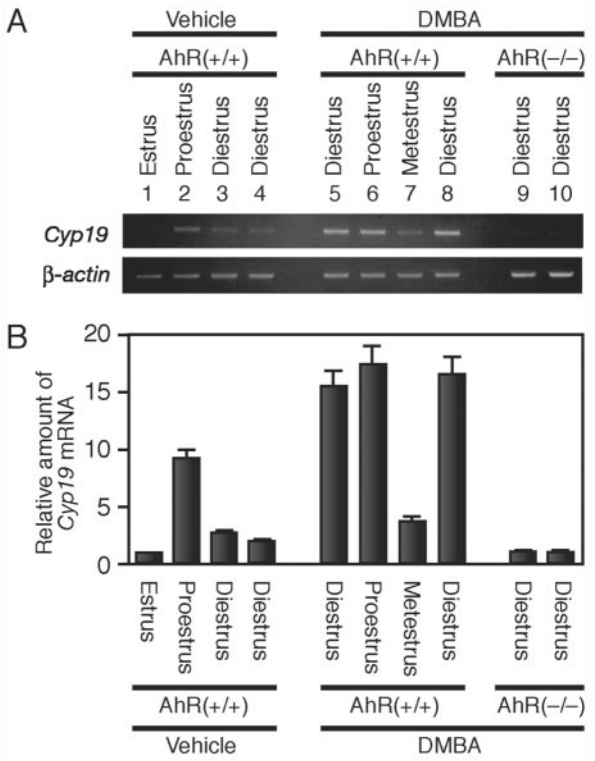

FIG. 7. Upregulation of *Cyp19* expression by an exogenous AhR ligand, DMBA. (A) Expression of *Cyp19* induced by intraperitoneal injection of DMBA. $AhR^{+/+}$ (lanes 1 to 8) or $AhR^{-/-}$ (lanes 9 and 10) female mice were injected intraperitoneally with DMBA (50 mg/kg of body weight) or vehicle alone. Five hours after injection, we prepared total RNA from the ovaries. The amounts of *Cyp19* mRNA were then evaluated by RT-PCR. The estrus cycle phase of each animal was determined by observing vaginal smears collected just before injection of DMBA. β-Actin was used as a control. (B) Quantitative representation of *Cyp19* mRNA levels. Quantification of the *Cyp19* transcript was performed by using a 7500 real-time PCR system (Applied Biosystems, Japan).

ple reactions in the ovary. Investigation of steroidogenic gene expression revealed that *Cyp19* expression was significantly reduced in $AhR^{-/-}$ females. Immunohistochemical and immunoblotting analyses confirmed the reduced levels of Cyp19 in granulosa cells. As Cyp19 is the rate-limiting enzyme in estrogen synthesis, it is likely that the reduced estradiol concentrations result primarily from lower levels of Cyp19 synthesis in the ovaries of $AhR^{-/-}$ females.

The *Cyp19* gene has multiple tissue-specific first exons (23, 33, 55). A survey of the 5′ sequence upstream of the ovary-specific first exon revealed the presence of a potential XRE sequence in both human and mouse genes. The presence of such an XRE sequence has recently been reported to occur within the promoter of the fish ovarian-type *CYP19* genes, although a functional analysis remains to be performed (7, 27, 59, 60). The conservation of XRE among a variety of animal species, however, suggests functionality of this sequence in the ovary-specific expression of *Cyp19*. In this study, we substantiated this hypothesis by transient transfection and ChIP assays. In addition, the *Cyp19* gene proximal promoter contained a functional Ad4/SF-1 site (32). Our investigation of the functional correlation between Ad4BP/SF-1 and AhR revealed that these factors cooperatively enhanced *Cyp19* gene transcription. This synergistic action resulted from a physical interaction, revealed by coimmunoprecipitation and ChIP assays.

Recently, another orphan nuclear receptor, LRH-1 (*l*iver *r*eceptor *h*omologue 1), has been reported to be selectively expressed in ovarian granulosa cells (15, 24) and to transactivate the ovary-specific *Cyp19* promoter in transient transfection assays. Structurally, LRH-1 exhibits homology with Ad4BP/SF-1, and the recognition sequences of these proteins are quite similar. Using the Ad4/SF-1 site from the *Cyp19* promoter as a probe, however, electrophoretic mobility shift assays revealed that Ad4BP/SF-1 is the dominant binding factor (9, 10, 15). These observations suggest that Ad4BP/SF-1 and LRH-1 play distinct roles in the regulation of target gene transcription. As LRH-1 is involved in cell proliferation via regulation of cyclin D1 and E1 gene expression (5), further investigations are needed to clarify the function of LRH-1 in the AhR-mediated expression of *Cyp19* in the ovary.

Role of negative feedback regulatory loop formed by AhR and AhRR. AhRR is one of the downstream targets of AhR transcriptional regulation (2, 36). Structurally, AhRR belongs to a family of bHLH-PAS transcription factors and suppresses AhR-mediated transactivation by competing with AhR for heterodimer formation with Arnt. This study confirmed the suppressive function of AhRR on *Cyp19* gene expression. The expressions of both AhRR and *Cyp19* are similarly regulated by AhR via binding of AhR to the XRE sequences in their promoters. Superovulation experiments, however, revealed that the *Cyp19* gene displayed an earlier peak of expression (reaching a maximum at 48 to 52 h after gonadotropin [PMSG] treatment) than AhRR, which was upregulated as *Cyp19* expression began to decline. Although the mechanisms producing this time lag of AhRR expression are unknown, cyclic expression of *Cyp19* in the estrus cycle could be explained by a lag in AhRR synthesis. From these observations, it is possible that AhR and AhRR regulate the ovarian biological clock governing the estrus cycle. In support of this possibility, it is interesting to note that expression of CLOCK and BMAL1 (Arnt3), two members of the bHLH-PAS family (to which AhR and AhRR belong), in the suprachiasmatic nuclei of the hypothalamus regulates the expression of their inhibitors, PERs, to generate the biological clock governing circadian rhythms (31).

In a normal ovarian cycle, the expression levels of AhR appear to be constant. Thus, to transactivate the expression of *Cyp19* and AhRR, AhR may also need to be activated. Although a number of endogenous ligands have been reported to activate AhR (13), the identity of the endogenous ligand required for the activation of AhR in the ovary and the mechanism by which this activation occurs during the estrus cycle remains unknown. In keratinocyte cell lines cultured at low density or in Ca^{2+}-free medium, AhR translocates to the nucleus to activate reporter genes, even in the absence of obvious AhR ligands (25). The activation of AhR by phosphorylation has been suggested for such cases (26).

Estrogenic effect of AhR ligand through two distinct mechanisms. In this study, we characterized the subfertility phenotype of $AhR^{-/-}$ female mice, identifying the key role of AhR in *Cyp19* gene transcription controlling the temporal synthesis

of ovarian estrogen in the estrus cycle. This intrinsic physiological role of AhR provides an explanation for the high degree of AhR conservation throughout vertebrate species. This finding also provides a molecular basis for the estrogenic actions of AhR ligands. DMBA, an AhR ligand, induced *Cyp19* expression, leading to unscheduled increases in estradiol regardless of estrus cycle phase. Recently, functional cross talk was reported between AhR and estrogen receptors (ER) (44), and the ligand-bound AhR exerts estrogenic effects through a direct interaction with nonliganded ER molecules associated with estrogen response elements in target gene promoters. Together with our observations, ligand-bound AhR likely exerts an estrogenic effect via two distinct mechanisms, the stimulation of estradiol production through the activation of *Cyp19* gene expression and the activation of empty ER by AhR coactivation.

ACKNOWLEDGMENTS

We thank R. S. Pollenz (University of South Florida) for kindly providing the AhR antibody and T. Etoh (Central Laboratories for Experimental Animals, Japan) for the care of laboratory mice. We are also grateful to Y. Nemoto for clerical work.

This work was funded in part by Core Research for Evolutionary Science and Technology, Solution Oriented Research for Science and Technology from Japan Science and Technology and Research Fellowship (T. Baba) of the Japan Society for the Promotion of Science for Young Scientists.

REFERENCES

1. **Abbott, B. D., J. E. Schmid, J. A. Pitt, A. R. Buckalew, C. R. Wood, G. A. Held, and J. J. Diliberto.** 1999. Adverse reproductive outcomes in the transgenic Ah receptor-deficient mouse. Toxicol. Appl. Pharmacol. **155:**62–70.
2. **Baba, T., J. Mimura, K. Gradin, A. Kuroiwa, T. Watanabe, Y. Matsuda, J. Inazawa, K. Sogawa, and Y. Fujii-Kuriyama.** 2001. Structure and expression of the Ah receptor repressor gene. J. Biol. Chem. **276:**33101–33110.
3. **Benedict, J. C., T. M. Lin, I. K. Loeffler, R. E. Peterson, and J. A. Flaws.** 2000. Physiological role of the aryl hydrocarbon receptor in mouse ovary development. Toxicol. Sci. **56:**382–388.
4. **Benedict, J. C., K. P. Miller, T. M. Lin, C. Greenfeld, J. K. Babus, R. E. Peterson, and J. A. Flaws.** 2003. Aryl hydrocarbon receptor regulates growth, but not atresia, of mouse preantral and antral follicles. Biol. Reprod. **68:** 1511–1517.
5. **Botrugno, O. A., E. Fayard, J. S. Annicotte, C. Haby, T. Brennan, O. Wendling, T. Tanaka, T. Kodama, W. Thomas, J. Auwerx, and K. Schoonjans.** 2004. Synergy between LRH-1 and beta-catenin induces G1 cyclin-mediated cell proliferation. Mol. Cell **15:**499–509.
6. **Brown, N. M., P. A. Manzolillo, J. X. Zhang, J. Wang, and C. A. Lamartiniere.** 1998. Prenatal TCDD and predisposition to mammary cancer in the rat. Carcinogenesis **19:**1623–1629.
7. **Callard, G. V., A. V. Tchoudakova, M. Kishida, and E. Wood.** 2001. Differential tissue distribution, developmental programming, estrogen regulation and promoter characteristics of *cyp19* genes in teleost fish. J. Steroid Biochem. Mol. Biol. **79:**305–314.
8. **Carlone, D. L., and J. S. Richards.** 1997. Functional interactions, phosphorylation, and levels of 3′,5′-cyclic adenosine monophosphate-regulatory element binding protein and steroidogenic factor-1 mediate hormone-regulated and constitutive expression of aromatase in gonadal cells. Mol. Endocrinol. **11:**292–304.
9. **Clyne, C. D., A. Kovacic, C. J. Speed, J. Zhou, V. Pezzi, and E. R. Simpson.** 2004. Regulation of aromatase expression by the nuclear receptor LRH-1 in adipose tissue. Mol. Cell. Endocrinol. **215:**39–44.
10. **Clyne, C. D., C. J. Speed, J. Zhou, and E. R. Simpson.** 2002. Liver receptor homologue-1 (LRH-1) regulates expression of aromatase in preadipocytes. J. Biol. Chem. **277:**20591–20597.
11. **Conn, P. M., J. G. Chafouleas, D. Rogers, and A. R. Means.** 1981. Gonadotropin releasing hormone stimulates calmodulin redistribution in rat pituitary. Nature **292:**264–265.
12. **Curtis Hewitt, S., E. H. Goulding, E. M. Eddy, and K. S. Korach.** 2002. Studies using the estrogen receptor alpha knockout uterus demonstrate that implantation but not decidualization-associated signaling is estrogen dependent. Biol. Reprod. **67:**1268–1277.
13. **Denison, M. S., and S. R. Nagy.** 2003. Activation of the aryl hydrocarbon receptor by structurally diverse exogenous and endogenous chemicals. Annu. Rev. Pharmacol. Toxicol. **43:**309–334.
14. **Dupont, S., A. Krust, A. Gansmuller, A. Dierich, P. Chambon, and M. Mark.** 2000. Effect of single and compound knockouts of estrogen receptors alpha (ERalpha) and beta (ERbeta) on mouse reproductive phenotypes. Development **127:**4277–4291.
15. **Falender, A. E., R. Lanz, D. Malenfant, L. Belanger, and J. S. Richards.** 2003. Differential expression of steroidogenic factor-1 and FTF/LRH-1 in the rodent ovary. Endocrinology **144:**3598–3610.
16. **Fero, M. L., M. Rivkin, M. Tasch, P. Porter, C. E. Carow, E. Firpo, K. Polyak, L. H. Tsai, V. Broudy, R. M. Perlmutter, K. Kaushansky, and J. M. Roberts.** 1996. A syndrome of multiorgan hyperplasia with features of gigantism, tumorigenesis, and female sterility in p27(Kip1)-deficient mice. Cell **85:**733–744.
17. **Fisher, C. R., K. H. Graves, A. F. Parlow, and E. R. Simpson.** 1998. Characterization of mice deficient in aromatase (ArKO) because of targeted disruption of the *cyp19* gene. Proc. Natl. Acad. Sci. USA **95:**6965–6970.
18. **Fujisawa-Sehara, A., K. Sogawa, M. Yamane, and Y. Fujii-Kuriyama.** 1987. Characterization of xenobiotic responsive elements upstream from the drug-metabolizing cytochrome P-450c gene: a similarity to glucocorticoid regulatory elements. Nucleic Acids Res. **15:**4179–4191.
19. **Gibbons, A.** 1993. Dioxin tied to endometriosis. Science **262:**1373.
20. **Hahn, M. E.** 2002. Aryl hydrocarbon receptors: diversity and evolution. Chem.-Biol. Interact. **141:**131–160.
21. **Hankinson, O.** 1995. The aryl hydrocarbon receptor complex. Annu. Rev. Pharmacol. Toxicol. **35:**307–340.
22. **Harada, N.** 1988. Novel properties of human placental aromatase as cytochrome P-450: purification and characterization of a unique form of aromatase. J. Biochem. (Tokyo) **103:**106–113.
23. **Harada, N., T. Utsumi, and Y. Takagi.** 1993. Tissue-specific expression of the human aromatase cytochrome P-450 gene by alternative use of multiple exons 1 and promoters, and switching of tissue-specific exons 1 in carcinogenesis. Proc. Natl. Acad. Sci. USA **90:**11312–11316.
24. **Hinshelwood, M. M., J. J. Repa, J. M. Shelton, J. A. Richardson, D. J. Mangelsdorf, and C. R. Mendelson.** 2003. Expression of LRH-1 and SF-1 in the mouse ovary: localization in different cell types correlates with differing function. Mol. Cell. Endocrinol. **207:**39–45.
25. **Ikuta, T., Y. Kobayashi, and K. Kawajiri.** 2004. Cell density regulates intracellular localization of aryl hydrocarbon receptor. J. Biol. Chem. **279:** 19209–19216.
26. **Ikuta, T., Y. Kobayashi, and K. Kawajiri.** 2004. Phosphorylation of nuclear localization signal inhibits the ligand-dependent nuclear import of aryl hydrocarbon receptor. Biochem. Biophys. Res. Commun. **317:**545–550.
27. **Kazeto, Y., S. Ijiri, A. R. Place, Y. Zohar, and J. M. Trant.** 2001. The 5′-flanking regions of CYP19A1 and CYP19A2 in zebrafish. Biochem. Biophys. Res. Commun. **288:**503–508.
28. **Kazlauskas, A., L. Poellinger, and I. Pongratz.** 1999. Evidence that the co-chaperone p23 regulates ligand responsiveness of the dioxin (aryl hydrocarbon) receptor. J. Biol. Chem. **274:**13519–13524.
29. **Kiyokawa, H., R. D. Kineman, K. O. Manova-Todorova, V. C. Soares, E. S. Hoffman, M. Ono, D. Khanam, A. C. Hayday, L. A. Frohman, and A. Koff.** 1996. Enhanced growth of mice lacking the cyclin-dependent kinase inhibitor function of p27(Kip1). Cell **85:**721–732.
30. **Komatsu, T., H. Mizusaki, T. Mukai, H. Ogawa, D. Baba, M. Shirakawa, S. Hatakeyama, K. I. Nakayama, H. Yamamoto, A. Kikuchi, and K. Morohashi.** 2004. Small ubiquitin-like modifier 1 (SUMO-1) modification of the synergy control motif of Ad4 binding protein/steroidogenic factor 1 (Ad4BP/SF-1) regulates synergistic transcription between Ad4BP/SF-1 and Sox9. Mol. Endocrinol. **18:**2451–2462.
31. **Lowrey, P. L., and J. S. Takahashi.** 2000. Genetics of the mammalian circadian system: photic entrainment, circadian pacemaker mechanisms, and posttranslational regulation. Annu. Rev. Genet. **34:**533–562.
32. **Lynch, J. P., D. S. Lala, J. J. Peluso, W. Luo, K. L. Parker, and B. A. White.** 1993. Steroidogenic factor 1, an orphan nuclear receptor, regulates the expression of the rat aromatase gene in gonadal tissues. Mol. Endocrinol. **7:**776–786.
33. **Means, G. D., M. W. Kilgore, M. S. Mahendroo, C. R. Mendelson, and E. R. Simpson.** 1991. Tissue-specific promoters regulate aromatase cytochrome P450 gene expression in human ovary and fetal tissues. Mol. Endocrinol. **5:**2005–2013.
34. **Meyer, B. K., and G. H. Perdew.** 1999. Characterization of the AhR-hsp90-XAP2 core complex and the role of the immunophilin-related protein XAP2 in AhR stabilization. Biochemistry **38:**8907–8917.
35. **Meyer, B. K., M. G. Pray-Grant, J. P. Vanden Heuvel, and G. H. Perdew.** 1998. Hepatitis B virus X-associated protein 2 is a subunit of the unliganded aryl hydrocarbon receptor core complex and exhibits transcriptional enhancer activity. Mol. Cell. Biol. **18:**978–988.
36. **Mimura, J., M. Ema, K. Sogawa, and Y. Fujii-Kuriyama.** 1999. Identification of a novel mechanism of regulation of Ah (dioxin) receptor function. Genes Dev. **13:**20–25.
37. **Mimura, J., and Y. Fujii-Kuriyama.** 2003. Functional role of AhR in the expression of toxic effects by TCDD. Biochim. Biophys. Acta **1619:**263–268.
38. **Mimura, J., K. Yamashita, K. Nakamura, M. Morita, T. N. Takagi, K. Nakao, M. Ema, K. Sogawa, M. Yasuda, M. Katsuki, and Y. Fujii-Kuriyama.**

1997. Loss of teratogenic response to 2,3,7,8-tetrachlorodibenzo-*p*-dioxin (TCDD) in mice lacking the Ah (dioxin) receptor. Genes Cells **2:**645–654.
39. **Mizusaki, H., K. Kawabe, T. Mukai, E. Ariyoshi, M. Kasahara, H. Yoshioka, A. Swain, and K. Morohashi.** 2003. *Dax-1* (dosage-sensitive sex reversal-adrenal hypoplasia congenita critical region on the X chromosome, gene 1) gene transcription is regulated by Wnt4 in the female developing gonad. Mol. Endocrinol. **17:**507–519.
40. **Morohashi, K., S. Honda, Y. Inomata, H. Handa, and T. Omura.** 1992. A common trans-acting factor, Ad4-binding protein, to the promoters of steroidogenic P-450s. J. Biol. Chem. **267:**17913–17919.
41. **Morohashi, K., U. M. Zanger, S. Honda, M. Hara, M. R. Waterman, and T. Omura.** 1993. Activation of CYP11A and CYP11B gene promoters by the steroidogenic cell-specific transcription factor, Ad4BP. Mol. Endocrinol. **7:**1196–1204.
42. **Nelson, J. F., L. S. Felicio, P. K. Randall, C. Sims, and C. E. Finch.** 1982. A longitudinal study of estrous cyclicity in aging C57BL/6J mice. I. Cycle frequency, length and vaginal cytology. Biol. Reprod. **27:**327–339.
43. **Nomura, M., K. Kawabe, S. Matsushita, S. Oka, O. Hatano, N. Harada, H. Nawata, and K. Morohashi.** 1998. Adrenocortical and gonadal expression of the mammalian Ftz-F1 gene encoding Ad4BP/SF-1 is independent of pituitary control. J. Biochem. (Tokyo) **124:**217–224.
44. **Ohtake, F., K. Takeyama, T. Matsumoto, H. Kitagawa, Y. Yamamoto, K. Nohara, C. Tohyama, A. Krust, J. Mimura, P. Chambon, J. Yanagisawa, Y. Fujii-Kuriyama, and S. Kato.** 2003. Modulation of oestrogen receptor signalling by association with the activated dioxin receptor. Nature **423:**545–550.
45. **Omura, T., and K. Morohashi.** 1995. Gene regulation of steroidogenesis. J. Steroid Biochem. Mol. Biol. **53:**19–25.
46. **Orlando, V., H. Strutt, and R. Paro.** 1997. Analysis of chromatin structure by in vivo formaldehyde cross-linking. Methods **11:**205–214.
47. **Pall, M., P. Hellberg, M. Brannstrom, M. Mikuni, C. M. Peterson, K. Sundfeldt, B. Norden, L. Hedin, and S. Enerback.** 1997. The transcription factor C/EBP-beta and its role in ovarian function; evidence for direct involvement in the ovulatory process. EMBO J. **16:**5273–5279.
48. **Parekh, B. S., and T. Maniatis.** 1999. Virus infection leads to localized hyperacetylation of histones H3 and H4 at the IFN-beta promoter. Mol. Cell **3:**125–129.
49. **Poland, A., E. Glover, and A. S. Kende.** 1976. Stereospecific, high affinity binding of 2,3,7,8-tetrachlorodibenzo-*p*-dioxin by hepatic cytosol. Evidence that the binding species is receptor for induction of aryl hydrocarbon hydroxylase. J. Biol. Chem. **251:**4936–4946.
50. **Poland, A., and J. C. Knutson.** 1982. 2,3,7,8-tetrachlorodibenzo-*p*-dioxin and related halogenated aromatic hydrocarbons: examination of the mechanism of toxicity. Annu. Rev. Pharmacol. Toxicol. **22:**517–554.
51. **Richards, J. S.** 1994. Hormonal control of gene expression in the ovary. Endocr. Rev. **15:**725–751.
52. **Richards, J. S.** 2001. Perspective: the ovarian follicle—a perspective in 2001. Endocrinology **142:**2184–2193.
53. **Robles, R., Y. Morita, K. K. Mann, G. I. Perez, S. Yang, T. Matikainen, D. H. Sherr, and J. L. Tilly.** 2000. The aryl hydrocarbon receptor, a basic helix-loop-helix transcription factor of the PAS gene family, is required for normal ovarian germ cell dynamics in the mouse. Endocrinology **141:**450–453.
54. **Roby, K. F.** 2001. Alterations in follicle development, steroidogenesis, and gonadotropin receptor binding in a model of ovulatory blockade. Endocrinology **142:**2328–2335.
55. **Sebastian, S., and S. E. Bulun.** 2001. A highly complex organization of the regulatory region of the human CYP19 (aromatase) gene revealed by the Human Genome Project. J. Clin. Endocrinol. Metab. **86:**4600–4602.
56. **Shimizu, Y., Y. Nakatsuru, M. Ichinose, Y. Takahashi, H. Kume, J. Mimura, Y. Fujii-Kuriyama, and T. Ishikawa.** 2000. Benzo[*a*]pyrene carcinogenicity is lost in mice lacking the aryl hydrocarbon receptor. Proc. Natl. Acad. Sci. USA **97:**779–782.
57. **Stanislaus, D., J. A. Janovick, T. Ji, T. M. Wilkie, S. Offermanns, and P. M. Conn.** 1998. Gonadotropin and gonadal steroid release in response to a gonadotropin-releasing hormone agonist in Gqalpha and G11alpha knockout mice. Endocrinology **139:**2710–2717.
58. **Sterneck, E., L. Tessarollo, and P. F. Johnson.** 1997. An essential role for C/EBPbeta in female reproduction. Genes Dev. **11:**2153–2162.
59. **Tchoudakova, A., M. Kishida, E. Wood, and G. V. Callard.** 2001. Promoter characteristics of two *cyp19* genes differentially expressed in the brain and ovary of teleost fish. J. Steroid Biochem. Mol. Biol. **78:**427–439.
60. **Tong, S. K., and B. C. Chung.** 2003. Analysis of zebrafish *cyp19* promoters. J. Steroid Biochem. Mol. Biol. **86:**381–386.
61. **Whitelaw, M., I. Pongratz, A. Wilhelmsson, J.-Å. Gustafsson, and L. Poellinger.** 1993. Ligand-dependent recruitment of the Arnt coregulator determines DNA recognition by the dioxin receptor. Mol. Cell. Biol. **13:**2504–2514.
62. **Yoshinaga-Hirabayashi, T., K. Ishimura, H. Fujita, J. Kitawaki, and Y. Osawa.** 1990. Immunocytochemical localization of aromatase in immature rat ovaries treated with PMSG and hCG, and in pregnant rat ovaries. Histochemistry **93:**223–228.